

Progress on SARS-CoV-2 3CLpro Inhibitors: Inspiration from SARS-CoV 3CLpro Peptidomimetics and Small-Molecule Anti-Inflammatory Compounds

Jiajie Zhu^{1,*}, Haiyan Zhang^{2,*}, Qinghong Lin¹, Jingting Lyu¹, Lu Lu¹, Hanxi Chen¹, Xuning Zhang¹, Yanjun Zhang³, Keda Chen¹

¹Shulan International Medical College, Zhejiang Shuren University, Hangzhou, People's Republic of China; ²Zhejiang Chinese Medical University, Hangzhou, People's Republic of China; ³Zhejiang Provincial Center for Disease Control and Prevention, Hangzhou, People's Republic of China

*These authors contributed equally to this work

Correspondence: Keda Chen, Shulan International Medical College, Zhejiang Shuren University, Hangzhou, People's Republic of China, Tel +8615068129828, Email Chenkd@zjsru.edu.cn; Yanjun Zhang, Zhejiang Provincial Center for Disease Control and Prevention, Hangzhou, People's Republic of China, Tel +8613858115856, Fax +86057188280783, Email yjzhang@cdc.zj.cn

Abstract: Coronavirus disease 2019 (COVID-19) caused by severe acute respiratory syndrome coronavirus 2 (SARS-CoV-2) currently poses a threat to human health. 3C-like proteinase (3CLpro) plays an important role in the viral life cycle. Hence, it is considered an attractive antiviral target protein. Whole-genome sequencing showed that the sequence homology between SARS-CoV-2 3CLpro and SARS-CoV 3CLpro is 96.08%, with high similarity in the substrate-binding region. Thus, assessing peptidomimetic inhibitors of SARS-CoV 3CLpro could accelerate the development of peptidomimetic inhibitors for SARS-CoV-2 3CLpro. Accordingly, we herein discuss progress on SARS-CoV-2 3CLpro peptidomimetic inhibitors. Inflammation plays a major role in the pathophysiological process of COVID-19. Small-molecule compounds targeting 3CLpro with both antiviral and anti-inflammatory effects are also briefly discussed in this paper.

Keywords: SARS-CoV, SARS-CoV-2, 3CLpro, peptidomimetics, anti-inflammatory agents, small-molecule inhibitors, protease inhibitors

Introduction

SARS-CoV and Middle East respiratory syndrome-Coronavirus (MERS-CoV) caused outbreaks of severe acute respiratory syndrome (SARS) in 2003 and Middle East respiratory syndrome (MERS) in 2012, respectively.¹⁻³ The dangers of these two viruses are well known. At the end of 2019, a dangerous novel coronavirus (SARS-CoV-2) was identified as the associated pathogen of a pneumonia outbreak in Wuhan, Hubei Province, China. Whole-genome sequencing showed that the sequence similarity between SARS-CoV-2 and the previous SARS-CoV was up to 79%, suggesting that the two viruses may share the same ancestor.⁴ However, with the virus sweeping the world, SARS-CoV-2 gradually displayed higher infectivity and the evolution of more mutant strains than SARS-CoV.⁵⁻⁸ In addition to vaccines, accelerating the development of antiviral drugs will benefit the long-term fight against SARS-CoV-2.

The virion of SARS-CoV-2 is composed of four major structural proteins; spike (S), nucleocapsid (N), membrane (M), and envelope (E) proteins (Figure 1A). Among them, S protein is divided into two functional units, S1 and S2. S1 promotes virus infection by binding to angiotensin-converting enzyme II (ACE2) of the host cell.⁹ N protein is also highly immunogenic and mainly forms nucleocapsid to protect viral RNA.¹⁰ These important structural proteins are derived from the translation and processing of the viral genome in the host cell. Therefore, preventing the generation of SARS-CoV-2 essential proteins could inhibit virus replication. 3Chymotrypsin-like protein (3CLpro) and papain-like protease (PLpro) are essential enzymes in the peptide chain processing reaction. They cleave the C-terminus of the

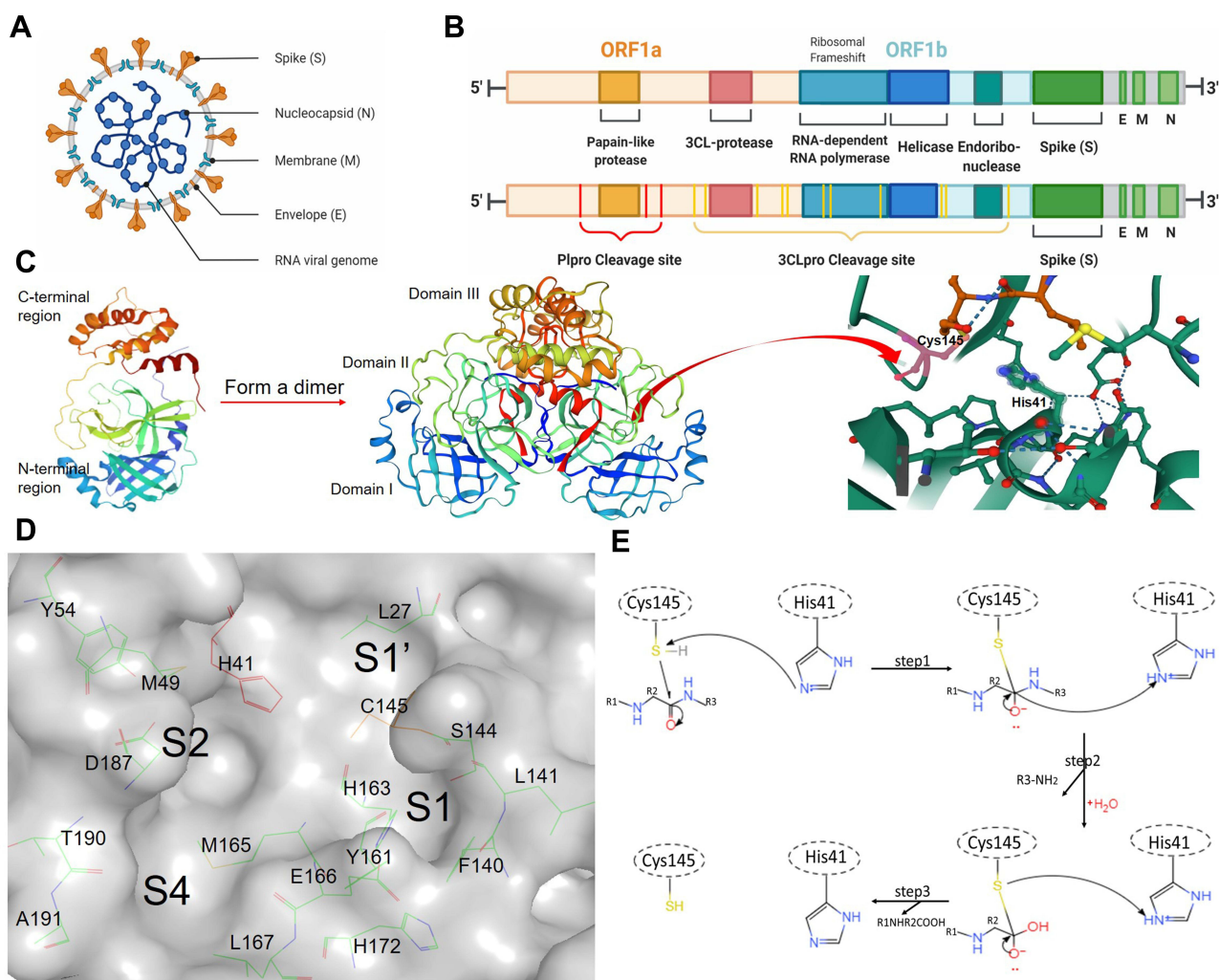


Figure 1 (A) Schematic diagram of Severe Acute Respiratory Syndrome Coronavirus 2 (SARS-CoV-2) morphology. (B) Papain-like protease (PLpro) and 3C-like proteinase (3CLpro) of cleavage site numbers of the polypeptide chain. (C) SARS-CoV-2 3CLpro 3D structure (monomer and dimer) and the N-terminal catalytic diad (His41-Cys145) (D). The substrate-binding pocket of SARS-CoV-2 3CLpro included S1'-S1-S2-S4 core sites. (E) SARS-CoV-2 3CLpro catalytic mechanism.

polypeptide chain at 11 sites and the N-terminus of the polypeptide chain at three sites, respectively.¹¹ The cleavage products include structural proteins and some important non-structural proteins, such as RNA-dependent RNA polymerase (RdRp) and helicase. With more cleavage sites than PLpro, 3CLpro has always been an attractive non-structural protein for the development of drugs targeting coronavirus.^{12,13} Recently, an oral SARS-CoV-2 3CLpro nitrile warhead peptidomimetic inhibitor (PF-07321332) was developed by Pfizer.¹⁴ PF-07321332 in combination with ritonavir is in Phase 2 and 3 clinical trials (NCT04960202 and NCT05011513) for treating SARS-CoV-2. Noticeably, PF-07321332 is optimized based on SARS-CoV 3CLpro peptidomimetic inhibitor PF-00835231.¹⁵ Importantly, sequence identity between SARS-CoV-2 3CLpro and SARS-CoV 3CLpro is 96%, with only 12 mutation points.¹⁶ This means that previous SARS-CoV 3CLpro peptidomimetic inhibitors are useful starting points for the design of SARS-CoV-2 antiviral drugs.

During the inflammatory phase of COVID-19, immune cells continue to express a large number of pro-inflammatory cytokines including interleukin 6 (IL-6), interferon gamma (IFN- γ), tumor necrosis factor (TNF), and chemokines due to over-activation of the patient's immune system.¹⁷ Cytokine storms can rapidly lead to acute respiratory distress syndrome (ARDS), pulmonary fibrosis consolidation, disseminated intravascular coagulation (DIC), and multiple organ failure.^{18,19} SARS-CoV-2-mediated cytokine storm is a major cause of death in critically ill patients. Although the role of 3CLpro in inflammatory immunity and COVID-19 is not as clear as that of PLpro, researchers have used substrate-targeted

proteomics and substrate screening techniques to reveal the complete substrate map of SARS-CoV-2 3CL protease.²⁰ 3CLpro can indirectly affect cytokine expression, and it can also specifically degrade Galectin-8 and thereby contribute to immune escape. Therefore, small-molecule anti-inflammatory drugs targeting 3CLpro may have a profound effect against COVID-19.

In this work, the structure and biological functions of SARS-CoV-2 3CLpro are described. In the second section, we review research progress on SARS-CoV-2 3CLpro peptide inhibitors based on the highly effective scaffolds of SARS-CoV peptide-like inhibitors. Finally, small-molecule inhibitors of SARS-CoV-2 3CLpro with anti-inflammatory effects are briefly summarized.

Crystal Structure and Biological Functions of SARS-CoV-2 3CLpro

After SARS-CoV-2 invades the host cell, the 29.8 kb positive-stranded RNA genome is released, which contains 14 open reading frames (ORFs) and encodes 27 proteins.^{21,22} When the reading frame of the ribosome is shifted to the -1 frame upstream of ORF1a through a sliding sequence (5'-UUUAAAC-3'), viral genome translation is initiated.²³ The 3' gene encodes the four structural proteins (S, E, M, N) and eight accessory proteins (3a, 3b, p6, 7a, 7b, 8b, 9b, orf14). The 5' gene is next to the 21.3kb ORF1 (ORF1a/b), which encodes pp1a (440–500 kDa) and pp1ab (740–810 kDa) polypeptides^{22,24,25}. Like Nsp5, 3CLpro (also named main protease, Mpro) is encoded by ORF1a, and it also participates in the cleavage of pp1ab via 11 conserved splicing sites¹¹ (Figure 1B). 3CLpro has three times more cleavage sites than PLpro, making it an ideal drug target.

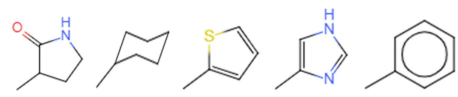
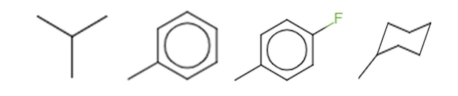
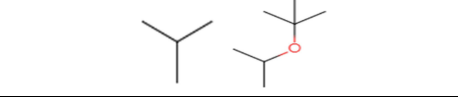
Crystal Structure

SARS-CoV-2 3CLpro consists of 306 amino acid residues, and it is a dimer (Figure 1C). Each monomer of the protease contains two regions; the N-terminal catalytic dyad region and the C-terminal region (Figure 1C). The N-terminal catalytic dyad is located in a cleft between chymotrypsin-like domains I (residues 8–101) and II (residues 102–184). The C-terminal region (domain III) contains five alpha-helices, and the globular folds formed by these helices are the basis for maintaining the structure of the active dimer of 3CLpro.¹⁶ Meanwhile, domain III (residues 201–303) is connected to domain II through a long flexible loop (residues 185–200), making the structure more flexible.²⁶ It is noteworthy that the two monomers are inserted into the C-terminal domain III at approximately right angles to each other. Therefore, any deflection of the C-terminal domain III of the dimer will affect its activity. For example, the R298A mutation of SARS-CoV 3CLpro causes domain III to rotate 33°, which disrupts the formation of dimers and reduces the catalytic activity. Thus, some drug studies targeting 3CLpro have focused on disrupting the dimer structure.^{27,28}

The Substrate-Binding Pocket and Biological Functions of SARS-CoV-2 3CLpro

The surface shape and the amino acid residue distribution of the substrate-binding pocket are especially important for studying the biological activity of enzymes and rationally designing structure-based small-molecule ligands. The protein lumen of the SARS-CoV-2 3CLpro substrate-binding channel contains six subsites (S1'–S5), which correspond to the P1'–P5 positions of the recognition sequence, respectively (Table 1). Among the six subsites, S1', S1, S2, and S4 are the four core sites and play a major role.²⁹ The amino acid species recognized by coronavirus 3CLpro at the S1', S1, S2, and S4 subsites are specific.^{29,30} This phenomenon is the same as the substrate specificity of picornavirus 3C protease.^{31,32} The characteristics of each subsite are critical to drug design. S1' is an important site of covalent warhead action, which contains the Cys145-His41 catalytic dyad. Cys145 functions as a nucleophile, while His41 acts as the proton donor/acceptor, participating in the catalytic process. The S1 and S2 binding subsites are two deep pockets. An oxyanion ring exists on the S1 subsite, which is an indispensable functional component of 3CLpro. The oxyanion ring can easily form hydrogen bonds with peptidomimetic inhibitors, which is mainly formed by the main chain nitrogen of Gly143, Ser144, and Cys145.³³ Meanwhile, the substrate peptide is conserved at the P1 position, and only Gln is selected^{12,34}. The imidazole group of His163 always interacts with the side chain of Gln through hydrogen bonding in the S1 subsite.¹² Therefore, the (S)- γ -lactam ring is a good substitution group for the Gln side chain. The S2 subsite is a flexible hydrophobic cavity, and the absence of any electron density was found to indicate the presence of ordered water in the S2 pocket.³⁵ The flexible side chain of Gln189 may be the key factor to

Table 1 Major Residues, Recognition Sequences, and High-Frequency Substituents of SARS-CoV-2 3CLpro Subsites

Subsites	Major Residues	Positions	Recognition Sequences	High-Frequency Substituents
S1'	L27, H41, Cys145	PI'	Ala, Ser, Gly, Asn	
S1	H163, E166, F140, G143, S144	PI	Gln	
S2	H41, M49, M165, Val186, D187, R188, Q189	P2	Leu, Phe, Met, Val	
S3	E166	P3	Thr, Lys, Arg, Val, Leu	
S4	M165, L167, Q189, T190, A191	P4	Ala, Val, Pro, Thr	
S5	T190, A191, Q192	P5	Val, Ala, Glu, Phe, Gly, His, Arg, Ser, Thr, Tyr	

Abbreviation: The international abbreviation for amino acids are used in this table.

preventing water from entering the S2 subsite when 3CLpro protease binds to different inhibitors.³⁵ Thus, S2 subsites favor hydrophobic amino acids, such as leucine.¹² Hydrophobic functional groups, such as a benzene ring and cyclopropyl-methyl, are usually selected when designing the P2 positions of peptidomimetic inhibitors. As a shallow hydrophobic pocket, the S4 subsite forms a narrow cavity. The P4 site always includes smaller amino acids (Ala, Val, Pro, and Thr). Therefore, researchers consider that these four subsites are major active sites. The S1'-S1-S2-S4 core sites include Leu27, His41, Met49, Ile51, Tyr54, Phe140, Leu141, Ser144, Cys145, Tyr161, His163, Met165, Glu166, Leu167, His172, Asp187, Thy190, and Ala191 residues^{16,34} (Figure 1D). In addition to His163, Glu166 also is an essential amino acid that recognizes substrate Gln-P1 and participates in hydrogen bond formation.³⁶ Glu166 of the other protomer is considered to interact with the N-finger of each of the two protomers, which can help form the S1 subsite of the substrate-binding pocket.³³ A study has shown that mutations of Glu166 will affect dimer aggregation.⁹ Meanwhile, the interactions between the two helices A' (residues 11–15) and other amino acids (Phe140, Met165, and His172) are also reported as major parts of the dimer.^{37,38} A shift in the backbone of amino acid residue (141–143) resulted in side-chain flipping of Asn142 upon binding of a peptidomimetic inhibitor at the S1 and S2 subsites. The flipped Asn142 acts as a half-gate to cover the S1 subsite. Met49 protrudes from the S2 subsite resulting in an upward shift of Gln189, which forms the other half of the gate and interacts with the P2 position of the substrate or inhibitor. Thus, Asn142, Met49, and Gln189 are considered to be substrate binding induced gate regulation switches at S1 and S2 subsites.³⁵

Unlike the traditional catalytic triad of chymotrypsin, the Cys145-His41 dimer constitutes the SARS-CoV-2 3CLpro catalytic site, which is located between S1' and S1 subsites.^{34,39} During the SARS-CoV-2 3CLpro catalytic process, the protonation state of the imidazole group of His41 leads to the formation of an ionized H41⁺—C145-dimer.⁴⁰ The deprotonated Cys145-thiol is highly nucleophilic and attacks the carbonyl carbon of the scissile bond in the substrate peptide plane. After nucleophilic attack, the N-terminal substrate fragment is released from the enzyme, and a thioester is formed between the enzyme's sulfhydryl group and the carbonyl group at the substrate's cleavage site. Next, the thioester is hydrolyzed by nucleophilic attack of a deprotonated water molecule, the corresponding C-terminal substrate fragment is released, and free enzyme is regenerated.^{41,42} The flowchart is shown in Figure 1E. In addition to the Cys145-His41 catalytic dyad, a water molecule (H₂O_{cat}) is also involved in the catalytic process by maintaining the protonation state of His41.⁴³ H₂O_{cat} forms hydrogen bonds with the side chains of His41, His164, and Asp187 to stabilize their positions. H₂O_{cat} buried beneath the surface of the protein is often missing due to

experimental conditions. Therefore, it is believed that using the room temperature structure of the SARS-CoV-2 3CLpro apo form may be a better solution for drug design. Unlike the free state of SARS-CoV-2 3CLpro, the biologically active conformation of the inhibitor-containing protease allows flexible allosteric action in the active site due to substrate-induced fit. This point needs to be considered and compared when establishing quantitative structure-bioactivity relationship (QSAR) models of drug molecules based on three-dimensional structures of proteins.

Using SARS-CoV Peptide-Like Inhibitors as Highly Effective Scaffolds

Based on the mechanism of coronavirus 3CLpro, the cleavage process of P4-P3-P2-P1-↓-P1' implies that simulating the chemical structure characteristics of C-terminal segments of substrate peptides holds promise.⁴² However, it is very difficult to develop molecular drug scaffolds based on the SARS-CoV-2 structure in the short term. In addition to 96.08% sequence similarity, direct protein skeleton registration analysis, also called the root mean square deviation (RMSD method), showed that SARS-CoV-2 3CLpro and SARS-CoV 3CLpro structures were also highly similar, with an RMSD difference of only 0.884 Å.¹⁶ This means that SARS-CoV 3CLpro peptidomimetic inhibitors based on different inhibitory mechanisms could provide valuable insights into the study of drugs that target the SARS-CoV-2 3CLpro active site.

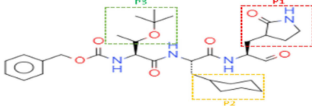
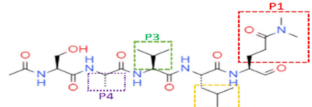
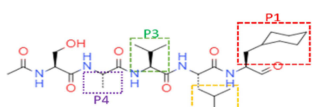
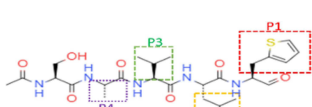
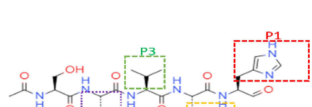

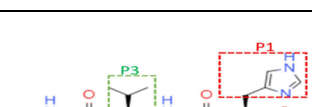


Peptide Aldehydes

The mercaptan of the Cys145-His41 dimer plays an important role in the enzymatic reaction of coronavirus 3CLpro. As electrophilic functional groups, aldehydes can undergo nucleophilic addition to mercaptan to form stable hemimercaptol.⁴⁴ Therefore, peptide aldehydes containing aldehyde warheads are potent inhibitors of 3CLpro.⁴⁵ In 2006, an effective SARS-CoV 3CLpro tripeptide aldehyde inhibitor, TG-0205221, was reported. TG-0205221 was stable in human plasma and could decrease the virus titer by 4.7Log10 in vitro at a dose of 5µm. The side chains at P1-P2-P3-P4 of TG-0205221 are (S)-γ-lactam ring, cyclohexyl, tertbutyl, and benzoxy groups⁴⁶ (Table 2). (S)-γ-lactam ring showed strong binding characteristics with S1 subsite and formed three hydrogen bonds in His163, Phe140, and Glu166.⁴⁶ The S2 subsite of 3CLpro is surrounded by hydrophobic amino acids, such as His41, Met165, and Met49. Thus, the hydrophobicity of the S2 subsite is considered. Five out of six in total cyclohexyl carbon atoms form extensive hydrophobic interactions with the S2 subsite.⁴⁶ In addition, the stable chair form of cyclohexyl makes it insert deeper into the S2 subsite. Benzoxy is locked to the S4 subsite in a folded conformation with the phenyl ring parallel to the wall-shaped region around A191 and the methylene group situated in the small corner.⁴⁶ The interaction between benzoxy and the S4 subsite is mainly hydrophobic interaction. Four of the six carbon atoms in the benzene ring have hydrophobic contact with the surrounding amino acid residues. Tertbutyl has a unique effect, which forms a hydrophobic interaction with the benzene ring of benzoxy. This acting force brings the backbone into tight contact with the S3 and S4 subsites and stabilizes three hydrogen-bonding interactions with Glu166 and Gln189.⁴⁶

In 2011, Akaji et al reported further progress on SARS-CoV 3CLpro tetrapeptide aldehyde inhibitors^{41,47} (compounds 1–5, Table 2). The results showed that the imidazolyl group was another effective substitution group for the P1 position (compounds 4 vs compounds 1–3), and selection of the cyclohexyl group for the P2 position was conducive to the complete occupation of the S2 subsite (compound 4 vs compound 5). Furthermore, the S4 subsite may engage in additional interactions with aldehydes through hydrogen bonding. Hence, it is better to select groups with hydrogen bonding receptors at the P4 site. In response to these points, further structural optimization afforded an effective tetrapeptide aldehyde inhibitor (compound 6, Table 2). In addition to peptidomimetic inhibitors with long peptides, aldehyde cinnamoyl benzene-benzene dipeptide (Cm-FF-H), a short peptide inhibitor, achieved good inhibition of SARS-CoV with a K_i value of $2.24 \pm 0.58 \mu\text{M}$ ⁴⁸ (Table 2). Almost all peptide-like inhibitors of 3CLpro choose to design an appropriate hydrophobic group at the P2 position.^{48–51} As a popular hydrophobic group, the rigid planar benzene ring was selected in the P2 position of Cm-FF-H.

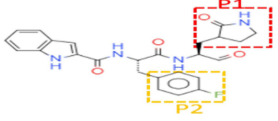
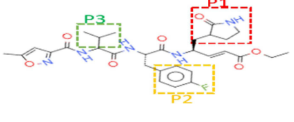
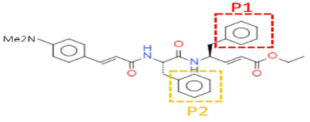
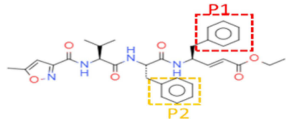
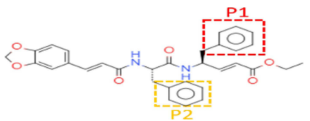
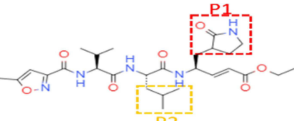
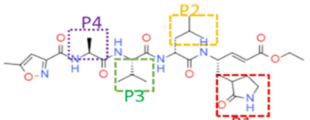
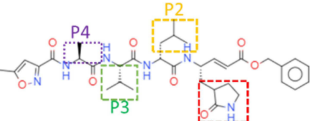
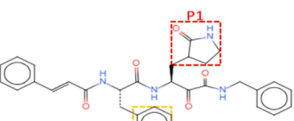
After the COVID-19 outbreak, Dai et al conducted preliminary research on SARS-CoV-2 3CLpro aldehyde inhibitors and identified an attractive inhibitor (compound 11a) using a short peptide scaffold similar to Cm-FF-H (Table 2).⁴⁹ The 50% inhibitory concentration (IC50) and EC50 values were $0.053 \pm 0.005 \mu\text{M}$ and $0.53 \pm 0.01 \mu\text{M}$, respectively. Good pharmacokinetics and low cytotoxicity were also observed. Crystal structure analysis of the SARS-CoV-2 3CLpro

Table 2 Details of SARS-CoV-2 and SARS-CoV 3CLpro Peptide-Like Inhibitors

Inhibitor	Structure	Antiviral Potency	Pharmacokinetic Characteristics
TG-0205221 (PDB: 2GX4) ⁴⁶		Anti-SARS-CoV: IC ₅₀ = 0.6 μM	TG-0205221 displays a relatively stable profile in mouse, rat, and human plasma
Compound 1 ⁴⁷		Anti-SARS-CoV: IC ₅₀ = 37 μM	NK
Compound 2 ⁴⁷		Anti-SARS-CoV: IC ₅₀ = 62 μM	NK
Compound 3 ⁴⁷		Anti-SARS-CoV: IC ₅₀ = 48 μM	NK
Compound 4 ⁴⁷		Anti-SARS-CoV: IC ₅₀ = 5.7 μM	NK
Compound 5 ⁴⁷		Anti-SARS-CoV: IC ₅₀ = 0.065 μM	NK
Compound 6 ⁴⁷		Anti-SARS-CoV: IC ₅₀ = 0.098 μM	NK
Cm-FF-H (PDB: 3SN8) ⁴⁸		Anti-SARS-CoV 3CLpro: K _i = 2.24 ± 0.58 μM	NK
Compound 11a (PDB: 6LZE) ⁴⁹		Anti-SARS-CoV-2: IC ₅₀ = 0.053 ± 0.005 μM EC ₅₀ = 0.53 ± 0.01 μM	CC ₅₀ > 100 μm (intravenously, 5 mg/kg) T _{1/2} = 4.41 h CL = 17.4 mL/min/mg

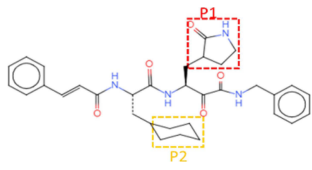
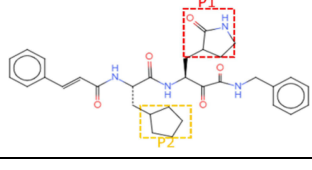
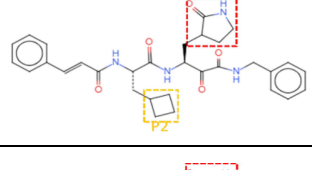
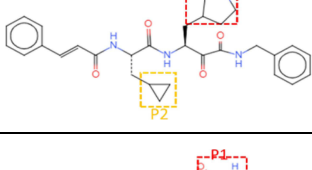
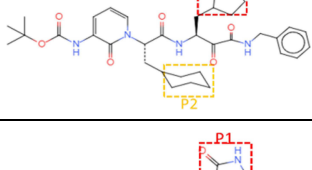
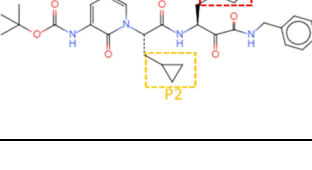
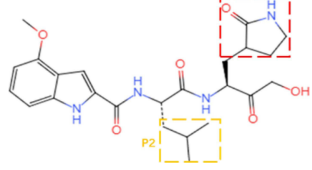
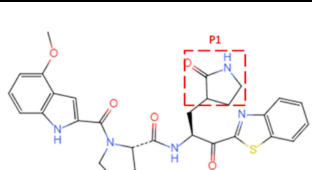
(Continued)

Table 2 (Continued).

Inhibitor	Structure	Antiviral Potency	Pharmacokinetic Characteristics
Compound 11b (PDB: 6M0K) ⁴⁹		Anti-SARS-CoV-2: IC ₅₀ = 0.040 ± 0.002 μM EC ₅₀ = 0.72 ± 0.09 μM	CC ₅₀ >100 μM (intravenously, 5 mg/kg) T _{1/2} = 1.65 h CL = 20.6 mL/min/mg
AG7088 ⁵⁰		Anti-SARS-CoV: IC ₅₀ >100 μM	NK
JMF1521 ⁵⁰		Anti-SARS-CoV: IC ₅₀ = 1 μM	NK
Compound 7 ⁵⁰		Anti-SARS-CoV: IC ₅₀ = 13 μM	NK
Compound 8 ⁵⁰		Anti-SARS-CoV: IC ₅₀ = 7 μM	NK
Compound 9 ⁴¹		Anti-SARS-CoV 3CLpro: K _i = 9.1 μM	NK
NI (PDB: 1WOF) ⁵²		Anti-SARS-CoV 3CLpro: K _i = 10.7 ± 1 μM	NK
N3 (PDB: 6LU7) ⁵³		Anti-SARS-CoV 3CLpro: K _i = 9.0 ± 0.8 μM Anti-SARS-CoV-2: EC ₅₀ = 16.77 ± 1.70 μM	CC ₅₀ >133 μM
Compound 10 (PDB: 5NI9) ⁵¹		Anti-SARS-CoV: IC ₅₀ = 1.95 ± 0.24 μM	NK

(Continued)

Table 2 (Continued).

Inhibitor	Structure	Antiviral Potency	Pharmacokinetic Characteristics
Compound 12 ⁵¹		Anti-SARS-CoV: IC ₅₀ = 0.71 ± 0.36 μM	NK
Compound 13 ⁵¹		Anti-SARS-CoV: IC ₅₀ = 1.27 ± 0.34 μM	NK
Compound 14 ⁵¹		Anti-SARS-CoV: IC ₅₀ = 1.44 ± 0.4 μM	NK
Compound 15 (PDB: 5N5O) ⁵¹		Anti-SARS-CoV: IC ₅₀ = 0.24 ± 0.08 μM	NK
Compound 16 ⁵⁶		NK	T _{1/2} = 1 h Clint _{human} = 21.0 μL min ⁻¹ (mg protein) ⁻¹ C _{max} = 334.5 ng mL ⁻¹
Compound 17 (PDB: 6Y2F) ⁵⁶		Anti-SARS-CoV-2: IC ₅₀ = 0.67 ± 0.18 μM Anti-SARS-CoV: 0.90 ± 0.29 μM	T _{1/2} = 1.8 h (mice) C _{max} = 126.2 ng mL ⁻¹ Plasma binding rate = 90%
PF-00835231 (PDB: 6XHM) 15		Anti-SARS-CoV-2 3CLpro: K _i = 0.271 nM	Clint (μL/min/mg) = 7.47 ± 0.88 Rat CL _p (mL/min/kg) = 27 ± 3.1 Oral F (%) = 1.4 ± 0.8 Fa × Fg (%) = 3.3
Compound 18 (PDB: 7RFR) 15		Anti-SARS-CoV-2 3CLpro: K _i = 230 nM	Clint (μL/min/mg) = 337 ± 9

(Continued)

Table 2 (Continued).

Inhibitor	Structure	Antiviral Potency	Pharmacokinetic Characteristics
Compound 19 (PDB: 7RFU) 15		Anti-SARS-CoV-2 3CLpro: Ki = 7.93 nM	Clint ($\mu\text{L}/\text{min}/\text{mg}$) = 127 ± 3 Rat CLp ($\text{mL}/\text{min}/\text{kg}$) = 42.9 Oral F (%) = 10 Fa \times Fg (%) = 84
Compound 20 15		Anti-SARS-CoV-2 3CLpro: Ki = 12.1 nM	Clint ($\mu\text{L}/\text{min}/\text{mg}$) = 30.3 ± 0.6 Rat CLp ($\text{mL}/\text{min}/\text{kg}$) = 31 Oral F (%) = 33 Fa \times Fg (%) = 100
PF-07321332 (PDB: 7RFS) 15		Anti-SARS-CoV-2 3CLpro: Ki = 3.11 nM	Clint ($\mu\text{L}/\text{min}/\text{mg}$) = 24.5 ± 0.2 Rat CLp ($\text{mL}/\text{min}/\text{kg}$) = 27.2 Oral F (%) = 50 Fa \times Fg (%) = 95

Abbreviations: Clint, Intrinsic clearance rate; CLp, plasma clearance rate; Oral F, oral bioavailability F; Fa \times Fg, fraction of oral dose absorbed from the gastrointestinal tract; Cmax, peak blood drug concentration; $T_{1/2}$, half-life.

complex containing compound 11a at 1.5 Å resolution showed that a stable 1.8 Å carbon-sulfur covalent bond is formed between the thiol S of Cys145 and the carbonyl C of the aldehyde warhead (the standard bond length of C-S bond is 1.82 Å). The oxygen of the carbonyl group interacts with the backbone NH of the Cys145 residue through a 2.9 Å hydrogen bond. On the C-terminal peptide-like fragment, the same (S)- γ -lactam ring and cyclohexyl group were selected at the P1 position and P2 position of compound 11a. The crystal structure showed that the (S)- γ -lactam ring matched well with the S1 subsite, and the cyclohexyl group stacked against the imidazole ring of His41 to stabilize the binding of compound 11a. In addition, indoles were incorporated at the P3 position to form hydrogen bonds with S4 in line with previous structural optimization, thereby improving drug properties. Figure 2A–C shows the binding mode between compound 11a and SARS-CoV-2 3CLpro.

Michael Acceptors

By conjugating olefinic or acetylenic bonds to electron-withdrawing groups, Michael acceptors have strong electrophilicity and they readily undergo nucleophilic addition reactions with sulfhydryl groups in cysteine residues.⁵² This results in one of the effective covalent warheads of 3CLpro. In 2005, AG7088, a ketomethyl isostere of a tripeptide-conjugated ester, was first proposed as a drug design model for anti-SARS-CoV 3CLpro Michael receptor inhibitors (Table 2).⁵⁰ Shie et al performed a series of optimizations on the P1-P2 positions of AG7088 by combinatorial chemistry and computer docking.⁵⁰ The (S)- γ -lactam ring and fluorophenyl group at P1-P2 positions of AG7088 were replaced by two phenyl groups. At the same time, the 4-(dimethylamino) cinnamyl group was selected to replace the isoxazole group at the N-terminus of the peptide to solve the steric hindrance problem. Among the optimized compounds, JMF1521 and compounds 7 and 8 displayed ideal inhibitory effects on SARS-CoV⁵⁰ (Table 2). Interestingly, one study showed that

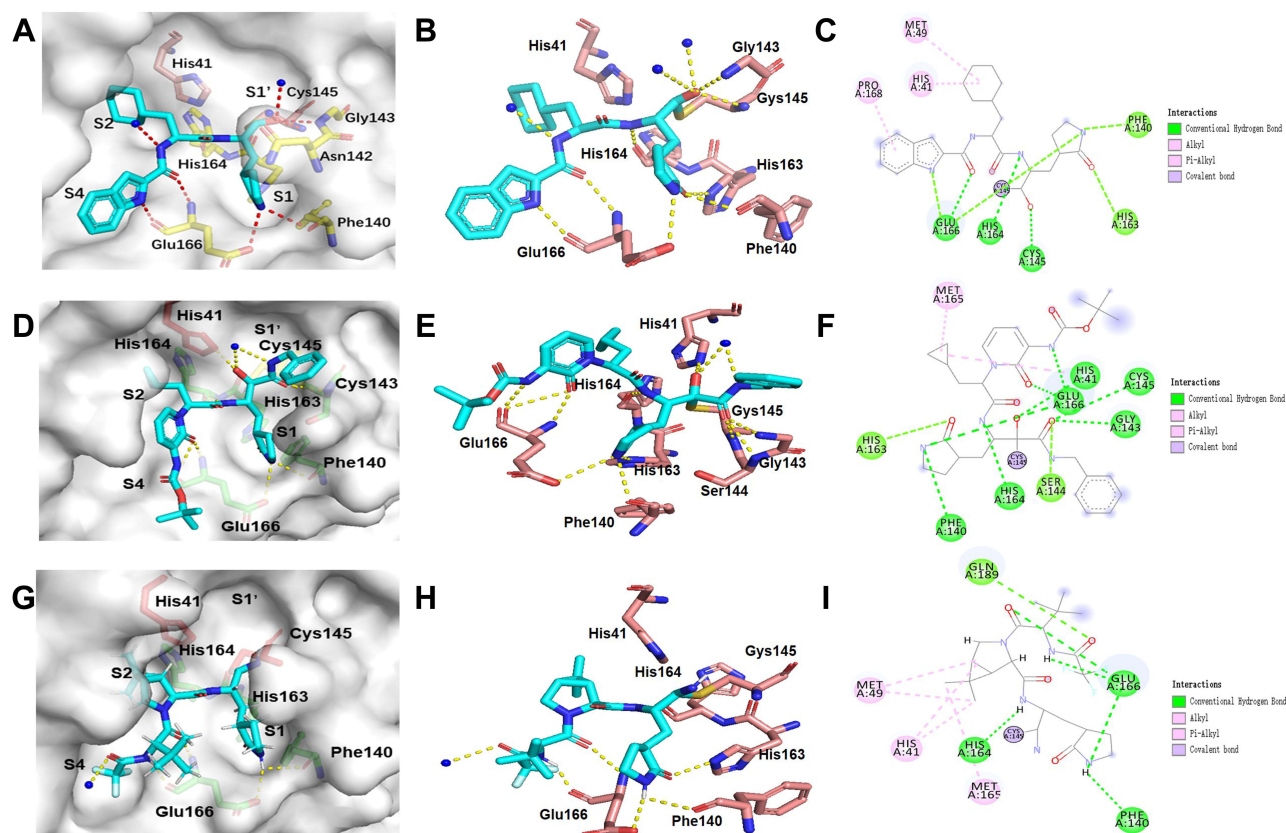


Figure 2 Inhibitor binding to SARS-CoV-2 3CLpro. Dashed lines in the three dimensions (3D) crystal models represent hydrogen bonds. (A–C) The binding mode between compound 11a and SARS-CoV-2 3CLpro. (D–F) The binding mode between compound 17 and SARS-CoV-2 3CLpro. (G–I) The binding mode between PF-07321332 and SARS-CoV-2 3CLpro. This figure was produced using PyMOL and Discovery Studio.⁸⁷

hydrophobic isopropyl groups at the P2 position had a stronger inhibitory effect than rigid flat groups (compound 9 vs AG7088, Table 2).⁴¹ Isopropyl groups may be more flexible.

Based on a previous SARS-CoV 3CLpro peptidomimetic inhibitor derivative library, Yang et al rationally designed three Michael receptor tetrapeptide inhibitors (N1, N9, and N3; Table 2).⁵² Surprisingly, N3 also showed specific antiviral activity against SARS-CoV-2, and its half-maximum effective concentration (EC₅₀) was $16.77 \pm 1.70 \mu\text{M}$. At the same time, a 50% cytotoxic concentration (CC₅₀) >133 μm confirmed low cytotoxicity of N3.⁵³ The crystal structure of the SARS-CoV-2 3CLpro complex containing N3 at 2.1 Å resolution showed that the C β atom of the N3 vinyl bond and the thiol of Cys145 formed a 1.8 Å covalent bond through an addition reaction. At the P1 position of N3, the lactam ring was used to replace the Gln side chain to occupy the S1 subsite, and a 2.4 Å hydrogen bond was formed with His163. P2, P3, and P4 positions retained the conserved Leu, Val, and Ala side chains of substrate peptides, respectively. The P2 residue is deeply inserted into the hydrophobic S2 subsite. The P4 position is firmly surrounded by Met165 and Leu167 side chains that stabilize N3. Isoxazole at the N-terminus interacts with the backbone of Pro168 via van der Waals forces.

α -Ketoamide Inhibitors

As an electrophilic warhead, α -ketoamide is more spatially applicable than aldehyde warheads and Michael acceptors. The α -ketoxy and amide oxygen result in α -ketoamide with two receptors for protein hydrogen bonds.⁵⁴ Nucleophilic attack by cysteine residues on the α -ketone carbon results in sulfhydryl hemiketals through competitive inhibition with substrates.⁵⁵ In response to the lack of commercial antiviral drugs for SARS-CoV, Zhang et al tried using α -ketoamide peptidomimetic inhibitors as anti-SARS-CoV inhibitors.⁵¹ They first synthesized compound 10 then made a series of compounds differing in the substituent at the P2 position. Substituents included cyclohexyl, cyclopentyl, cyclobutyl, and

cyclopropyl groups. Among them, cyclohexyl and cyclopropyl at the P2 position displayed good antiviral effects (compounds 12 and 15, Table 2). Cyclopropyl can alleviate steric hindrance and has better flexibility.

After the SARS-CoV-2 outbreak in December 2019, Zhang et al made further modifications on compound 12 and obtained compound 16 (Table 2).⁵⁶ Compound 16 hides the amide bond between the P2 position and the P3 position in the pyridone ring, which is a good solution to the problem of the Michael acceptor-type amide bond being easily degraded by plasma proteases. In terms of metabolic stability, compound 16 in human microsomes was moderately well with intrinsic clearance rates $Cl_{int_human} = 21.0 \mu\text{L}/\text{min}/\text{mg}$ protein.⁵⁶ At the same time, the less hydrophobic tert-butyl carbonyl group (Boc group) is used at the P3 position to enhance the water solubility of the compound. However, the cyclohexyl group at the P2 position of compound 16 is too large for the S2 subsite in 3CLpro, resulting in poor antiviral activity. Therefore, compound 17 uses a cyclopropyl group based on previous results⁵⁶ (Table 2). Its IC₅₀ value for SARS-CoV-2 3CLpro is $0.67 \pm 0.18 \mu\text{M}$. The crystal structure shows that Cys145 and α -ketone form a stable mercapto hemiketal. The hydroxyl and amide oxygen on the mercapto hemiketal engage in hydrogen bonds with other residues including His41 and Cys145, respectively. In addition, the (S)- γ -lactam ring at the P1 position and the cyclopropyl at the P2 position occupy their respective subsites in 3CLpro. At the same time, the pyridone at the P3-P2 positions occupies the main active site area of the virus's main protease, and the oxygen in its amide forms a hydrogen bond with Glu166. Compounds 16 and 17 are performed the subcutaneous administration in the CD-1 mice at 20 mg/kg and 3 mg/kg, respectively.⁵⁶ The plasma clearance rate of compound 16 was significantly higher than that of compound 17 (565.6 mL/kg/min Vs 131.6 mL/kg/min). This result is also reflected in the half-life and mean residence time (MRT) of these compounds after subcutaneous administration. The plasma half-life and the MRT of compound 16 were 1.0h and 1.6h. Compared with compound 16, the plasma half-life for compound 17 was extended to 1.8h and the MRT in mice was 2.7h. Furthermore, compound 17 was found to have a plasma protein binding ratio of 90%, so compound 16 had 3-folds the maximum plasma concentration (C_{max}) of compound 17 (334.5 ng/mL vs 126.2 ng/mL). However, the distribution properties of these compounds are roughly similar. Compounds 16 and 17 tend to be distributed to lung tissue, which helps them better fight SARS-CoV-2 infection. Figure 2D–F shows the binding mode between compound 17 and SARS-CoV-2 3CLpro.

PF-07321332

The clinical drug PAXLOVID™ is a novel coronavirus oral drug developed by Pfizer. Its main ingredient is PF-07321332. At present, PF-07321332 is the most successful example of using a SARS-CoV peptidomimetic inhibitor (PF-00835231) as a highly effective scaffold.¹⁵ PF-00835231 has a strong inhibitory effect on SARS-CoV-2 3CLpro and it is metabolically stable, but its passive absorptive permeability and oral availability are very low.^{57–59} Therefore, to obtain antiviral drugs with good pharmacokinetic properties, researchers replaced the covalent warhead and further optimized the side chain of the scaffold (Table 2, compounds 18–20).

In the optimization process, benzothiazole and nitrile group as covalent warheads significantly increase oral availability because more hydrogen bond donors (HBD) make the Michael acceptor reduce the oral bioavailability.¹⁵ Utilizing nitriles to reduce HBD count is the main difference between PF-07321332 and PF-00835231. In the side chain of the scaffold, the researchers also introduced a 6,6-dimethyl-3-azabicyclo hexane to simulate the cyclic Leu to further sweep the HBD from the P2/P3 amide linkage. This modification is similar to the local structure of the anti-HCV drug Boceprevir.⁶⁰ Compared with PF-00835231, this creative optimization can improve the passive absorptivity of PF-07321332 in Madin-Darby canine kidney-low efflux (MECK-LE) cells.¹⁵ Additionally, the N-terminal indole fragment was further changed to methylsulfonamide, which forms hydrogen bonds with both Gln189 and Glu166, and all indicators of drug function improved significantly (compound 18 vs compound 19). The branched and acyclic characteristics of methylsulfonamide helped peptidomimetics better fill S3 pockets of 3CLpro.¹⁵ Based on the interaction mode of methylsulfonamide, researchers developed compound 20 containing trifluoroacetamide. Although this measure reduces the antiviral potency of the inhibitor, but it greatly improves oral availability (compound 19 Vs compound 20). Finally, changing the benzothiazole of compound 20 to a -nitrile group yielded the clinical molecule PF-07321332. PF-07321332 and PF-00835231 showed significant differences in pharmacokinetics. The oral bioavailability and oral dose fraction absorbed from the gastrointestinal tract for PF-07321332 is 30 times higher than for PF-00835231 in the rats. In terms of drug metabolism, PF-07321332 and PF-00835231 expressed similar degrees of plasma clearance in rats (27.2 mL/min/kg Vs 27.0 mL/min/kg). However, PF-07321332 had an NADPH-dependent

metabolic clearance in liver microsomes about 3 times that of PF-00835231 due to the first-pass metabolism by CYP3A4. (24.5 $\mu\text{min}/\text{mg}$ Vs 7.47 $\mu\text{min}/\text{mg}$). Therefore, PF-07321332 is suggested to be used in combination with a potent CYP3A4 inhibitor (RTV) and the combination is positive in phase 2 and 3 clinical trials for COVID 19.^{15,61} Cytotoxicity of PF-07321332 and PF-00835231 was evaluated in the A549-ACE2 cell line. CC50 were $>100\mu\text{M}$ and $>10\mu\text{M}$, respectively.^{15,62} At the same time, PF-07321332 also has the advantages of facile large-scale synthesis, higher solubility, and reduced differential isomerization. Figure 2G–I shows the binding mode between PF-07321332 and SARS-CoV-2 3CLpro.

Anti-Inflammatory Small-Molecule Drugs Targeting 3CLpro

The new coronavirus infection is divided into three phases: a mild infection phase, a pulmonary phase, and an inflammation phase.⁶³ Antiviral and anti-inflammatory treatments in pulmonary and inflammatory phases are key to preventing the deterioration of patients with COVID-19 infection and ultimately saving lives. In this section, we discuss the profound implications of anti-inflammatory small-molecule drugs targeting 3CLpro.

Oxidative stress is the main factor in the pathophysiological process of SARS-CoV-2 infection.⁶⁴ Studies have shown that intake of selenium-rich foods can reduce virus replication and help reduce the rate of severe illness after SARS-CoV-2 infection.^{65,66} Ebselen is an organic selenium heterocyclic compound with similar enzymatic activity to glutathione peroxidase (GSH-PX).⁶⁷ Through its anti-biological oxidation effect, Ebselen can remove excess peroxides in the body, block the chain reaction that produces free radicals, and prevent obvious cell damage and immune dysfunction. Studies have shown that Ebselen can effectively treat lung diseases dominated by neutrophil infiltration, and it can also regulate some immune factors such as those mediated by IFN, IL-2, and TNF.^{68,69} Using high-throughput screening, Jin et al found that Ebselen has strong inhibitory activity against 3CLpro, with an IC50 of 0.67 μM .⁵³ Based on tandem mass spectrometry and inhibition data, Jin et al concluded that Ebselen may covalently bind to the catalytic dimer Cys145 of SARS-CoV-2 3CLpro, or it may inhibit 3CLpro through non-covalent binding. Recently, derivatives from Ebselen as a scaffold have been developed based on the SARS-CoV-2 3CLpro structure.⁷⁰

Natural products are a source of inspiration and resources for medicine. Many studies have shown that flavonoids play an active role in the anti-inflammatory and antiviral process of COVID-19 disease, and they are widely present in the roots, leaves, and fruits of plants in nature.^{71,72} The anti-SARS-CoV-2 effects of some flavonoids such as quercetin and proanthocyanidins have been widely reported.^{73,74} The inhibitory effects of two flavonoids (myricetin and dihydromyricetin) on SARS-CoV-2 3CLpro and their protective effects on lung inflammation were investigated,^{75,76} and the IC50 values were $3.684 \pm 0.076 \mu\text{M}$ and $1.716 \pm 0.419 \mu\text{M}$, respectively. Furthermore, using a mouse pneumonia model induced by bleomycin, results showed that myricetin and dihydromyricetin can inhibit the infiltration of inflammatory cells and the secretion of inflammatory cytokines IL-6, IL-1 α , TNF- α , and IFN- γ . Another flavonoid, Ugonin J (UJ), blocks the active site of SARS-CoV-2 3CLpro by forming hydrogen bonds with S1', S1, S2, and S4 subsites.⁷⁷ The EC50 of UJ against SARS-CoV-2 infection in Vero E6 cells was $2.38 \pm 0.9 \mu\text{M}$. Compared with the control group receiving anti-inflammatory drug dexamethasone (Dex), UJ downregulated the main pro-inflammatory factor IL-6 to a greater extent. In addition to flavonoids, Uras et al isolated butenolide I from the marine-derived fungus *Aspergillus terreus*, which effectively inhibited SARS-CoV-2 3CLpro proteases and exerted significant anti-inflammatory effects in vitro.⁷⁸ Andrographolide is an effective anti-inflammatory ingredient extracted from *Andrographis* with a wide range of biological activities. Shi et al found that andrographolide can inhibit the activity of SARS-CoV-2 3CLpro with an IC50 of $15.05 \pm 1.58 \text{ mM}$.⁷⁹

Conclusion and Perspectives

On November 9, 2021, a new SARS-CoV-2 variant (B.1.1.529) was detected for the first time in South Africa, and the World Health Organization (WHO) named it Omicron.⁸⁰ The Omicron strain contains 61 mutation sites, of which 32 are in the S protein, but the probability of mutation of 3CLpro still appears to be low.^{81,82} What is worrying is that the receptor-binding region of the S protein contains 10 mutation sites, which far exceeds the two mutations in the Delta variant.⁸⁰ Research indicates significant immune escape potential for the SARS-CoV-2 Omicron variant.⁸³ Therefore, in addition to research on next-generation vaccines and broad-spectrum vaccines, the development of targeted drugs for

SARS-CoV-2 3CLpro could prove valuable to the long-term struggle against this ever-changing viral pathogen. Currently, with the biological mechanism of SARS-CoV-2 *in vitro* and *in vivo* being elucidated, biological macromolecules and small molecules are two main types of anti-SARS-CoV-2 drugs. The former can treat COVID-19 patients by tending to act on targets on the surface of cells or viruses.^{84–86} Compared with macromolecules, small molecules are also more stable for resisting degradation and more likely to cross the cell membrane to target certain important proteases during viral replication, such as RNA-dependent RNA polymerase (RdRp) and 3CLpro. We focus on small molecules that have antiviral and antiinflammatory activity in this review.

In order to design high-affinity lead compounds, one strategy for enzyme inhibitor design is to mimic substrates or construct transition state analogs. To this end, the crystal structure of a protease, the substrate sequence, and the substrate recognition process can be harnessed to simulate the geometry and binding mode of the substrate in the enzyme-catalyzed reaction to reduce the enzymatic reaction rate or block catalysis completely. In this way, the design of peptidomimetic inhibitors based on the SARS-CoV-2 3CLpro structure could yield high-precision and high-affinity agents. Since the novel coronavirus outbreak, a number of peptide-like inhibitors have been designed using SARS-CoV peptide-like inhibitors as highly effective scaffolds.^{15,53,56} Given the high similarity between the substrate-binding pockets of SARS-CoV-2 and SARS-CoV 3CLpro, we believe that starting from some reported SARS-CoV peptide-like inhibitors, and identifying and modifying these scaffolds, could generate innovative scaffolds tailored to the SARS-CoV-2 3CLpro structure. This could avoid the development of peptidomimetic inhibitors based on natural substrates, and shorten the design and development of peptidomimetic inhibitors in general. Furthermore, similar to rational drug design, combinatorial chemistry systematically uses covalently connected building blocks, which can prepare a large number of compounds cost-effectively. Therefore, from an existing series of lead compounds, the design of new compounds by reorganizing the skeleton and substituent groups is a promising strategy for novel drug design. This strategy can also be used in the design of SARS-CoV-2 peptidomimetic inhibitors. In addition to replacing different covalent warheads, the groups at the main P1, P2, and P3 positions of peptidomimetic inhibitors can be replaced, and the groups most often used in these positions are summarized in [Table 1](#). This provides guidance for the reorganization and modification of the substitution groups of peptidomimetic inhibitors.

In addition to the development of peptidomimetic inhibitors, the use of high-throughput screening and molecular docking techniques for small-molecule compounds with SARS-CoV-2 3CLpro inhibitory properties is an established method for discovering new lead compounds. Small-molecule compounds with anti-inflammatory activity are particularly important. Natural compounds often have rich biological and antiviral activities, and many can help the body relieve extreme inflammatory responses and reduce the rate of severe diseases, as exemplified by flavonoids.⁷² Thus, molecular scaffolds based on these compounds have high drug potential. In addition to inhibiting the virus, they may participate in the potential regulatory network of inflammatory signals. Thus, designing derivatives based on these molecular scaffolds could prove fruitful.

Acknowledgments

I am profoundly grateful to my supervisor, Keda Chen, whose illuminating instruction and expert advice have guided me through every step of my writing of this review. His broad and profound knowledge gave me great impression as well as great help. My great gratitude also goes to some of my friends and classmates who have selfless and generously helped me with my thesis.

Funding

1. Supported by the opening foundation of the State Key Laboratory for Diagnosis and Treatment of Infectious Diseases, The First Affiliated Hospital, College of Medicine, Zhejiang University, grant NO. SKLID2020KF042.2. Supported by the Major horizontal project of Zhejiang Shuren University, grant NO. KHJ1720234.

Disclosure

The authors report no conflicts of interest in this work.

References

1. Ksiazek TG, Erdman D, Goldsmith CS, et al. A novel coronavirus associated with severe acute respiratory syndrome. *N Engl J Med.* 2003;348(20):1953–1966. doi:10.1056/NEJMoa030781
2. Li W, Shi Z, Yu M, et al. Bats are natural reservoirs of SARS-like coronaviruses. *Science.* 2005;310(5748):676–679. doi:10.1126/science.1118391
3. Lancet T. MERS-CoV: a global challenge. *Lancet.* 2013;381(9882):1960. doi:10.1016/S0140-6736(13)61184-8
4. Xu X, Chen P, Wang J, et al. Evolution of the novel coronavirus from the ongoing Wuhan outbreak and modeling of its spike protein for risk of human transmission. *Sci China Life Sci.* 2020;63(3):457–460. doi:10.1007/s11427-020-1637-5
5. Faria NR, Mellan TA, Whittaker C, et al. Genomics and epidemiology of a novel SARS-CoV-2 lineage in Manaus, Brazil. *medRxiv.* 2021;372:815–821.
6. Galloway SE, Paul P, MacCannell DR, et al. Emergence of SARS-CoV-2 B.1.1.7 lineage - United States, December 29, 2020–January 12, 2021. *MMWR Morb Mortal Wkly Rep.* 2021;70(3):95–99. doi:10.15585/mmwr.mm7003e2
7. Mlcochova P, Kemp SA, Dhar MS, et al. SARS-CoV-2 B.1.617.2 delta variant replication and immune evasion. *Nature.* 2021;599(7883):114–119. doi:10.1038/s41586-021-03944-y
8. Tegally H, Wilkinson E, Giovanetti M, et al. Detection of a SARS-CoV-2 variant of concern in South Africa. *Nature.* 2021;592(7854):438–443. doi:10.1038/s41586-021-03402-9
9. Lan J, Ge J, Yu J, et al. Structure of the SARS-CoV-2 spike receptor-binding domain bound to the ACE2 receptor. *Nature.* 2020;581(7807):215–220. doi:10.1038/s41586-020-2180-5
10. Perdikari TM, Murthy AC, Ryan VH, Watters S, Naik MT, Fawzi NL. SARS-CoV-2 nucleocapsid protein phase-separates with RNA and with human hnRNPs. *EMBO J.* 2020;39(24):e106478. doi:10.15252/embj.2020106478
11. Moustaqil M, Ollivier E, Chiu HP, et al. SARS-CoV-2 proteases PLpro and 3CLpro cleave IRF3 and critical modulators of inflammatory pathways (NLRP12 and TAB1): implications for disease presentation across species. *Emerg Microbes Infect.* 2021;10(1):178–195. doi:10.1080/22221751.2020.1870414
12. Anand K, Ziebuhr J, Wadhvani P, Mesters JR, Hilgenfeld R. Coronavirus main proteinase (3CLpro) structure: basis for design of anti-SARS drugs. *Science.* 2003;300(5626):1763–1767. doi:10.1126/science.1085658
13. Mody V, Ho J, Wills S, et al. Identification of 3-chymotrypsin like protease (3CLPro) inhibitors as potential anti-SARS-CoV-2 agents. *Commun Biol.* 2021;4(1):93. doi:10.1038/s42003-020-01577-x
14. Vandyck K, Deval J. Considerations for the discovery and development of 3-chymotrypsin-like cysteine protease inhibitors targeting SARS-CoV-2 infection. *Curr Opin Virol.* 2021;49:36–40. doi:10.1016/j.coviro.2021.04.006
15. Owen DR, Allerton CMN, Anderson AS, et al. An oral SARS-CoV-2 M(pro) inhibitor clinical candidate for the treatment of COVID-19. *Science.* 2021;374:eabl4784.
16. Gahlawat A, Kumar N, Kumar R, et al. Structure-based virtual screening to discover potential lead molecules for the SARS-CoV-2 main protease. *J Chem Inf Model.* 2020;60(12):5781–5793. doi:10.1021/acs.jcim.0c00546
17. McElvaney OJ, McEvoy NL, McElvaney OF, et al. Characterization of the inflammatory response to severe COVID-19 illness. *Am J Respir Crit Care Med.* 2020;202(6):812–821. doi:10.1164/rccm.202005-1583OC
18. Moore JB, June CH. Cytokine release syndrome in severe COVID-19. *Science.* 2020;368(6490):473–474. doi:10.1126/science.abb8925
19. Terpos E, Ntanasis-Stathopoulos I, Elalamy I, et al. Hematological findings and complications of COVID-19. *Am J Hematol.* 2020;95(7):834–847. doi:10.1002/ajh.25829
20. Pablos I, Machado Y, de Jesus HCR, et al. Mechanistic insights into COVID-19 by global analysis of the SARS-CoV-2 3CL(pro) substrate degradome. *Cell Rep.* 2021;37(4):109892. doi:10.1016/j.celrep.2021.109892
21. Srinivasan S, Cui H, Gao Z, et al. Structural genomics of SARS-CoV-2 indicates evolutionary conserved functional regions of viral proteins. *Viruses.* 2020;12(4). doi:10.3390/v12040360
22. Wu A, Peng Y, Huang B, et al. Genome composition and divergence of the novel coronavirus (2019-nCoV) originating in China. *Cell Host Microbe.* 2020;27(3):325–328. doi:10.1016/j.chom.2020.02.001
23. Panda PK, Arul MN, Patel P, et al. Structure-based drug designing and immunoinformatics approach for SARS-CoV-2. *Sci Adv.* 2020;6(28):eabb8097. doi:10.1126/sciadv.abb8097
24. Chan JF, Kok KH, Zhu Z, et al. Genomic characterization of the 2019 novel human-pathogenic coronavirus isolated from a patient with atypical pneumonia after visiting Wuhan. *Emerg Microbes Infect.* 2020;9(1):221–236. doi:10.1080/22221751.2020.1719902
25. Marra MA, Jones SJ, Astell CR, et al. The genome sequence of the SARS-associated coronavirus. *Science.* 2003;300(5624):1399–1404. doi:10.1126/science.1085953
26. Graziano V, McGrath WJ, Yang L, Mangel WF. SARS CoV main proteinase: the monomer-dimer equilibrium dissociation constant. *Biochemistry.* 2006;45(49):14632–14641. doi:10.1021/bi061746y
27. Shi J, Sivaraman J, Song J. Mechanism for controlling the dimer-monomer switch and coupling dimerization to catalysis of the severe acute respiratory syndrome coronavirus 3C-like protease. *J Virol.* 2008;82(9):4620–4629. doi:10.1128/JVI.02680-07
28. Wu CG, Cheng SC, Chen SC, et al. Mechanism for controlling the monomer-dimer conversion of SARS coronavirus main protease. *Acta Crystallogr D Biol Crystallogr.* 2013;69(Pt 5):747–755. doi:10.1107/S0907444913001315
29. Stoddard SV, Stoddard SD, Oelkers BK, et al. Optimization rules for SARS-CoV-2 M(pro) antivirals: ensemble docking and exploration of the coronavirus protease active site. *Viruses.* 2020;12(9):942. doi:10.3390/v12090942
30. Anand K, Palm GJ, Mesters JR, Siddell SG, Ziebuhr J, Hilgenfeld R. Structure of coronavirus main proteinase reveals combination of a chymotrypsin fold with an extra alpha-helical domain. *EMBO J.* 2002;21(13):3213–3224. doi:10.1093/emboj/cdf327
31. Bergmann EM, Mosimann SC, Chernaia MM, Malcolm BA, James MN. The refined crystal structure of the 3C gene product from hepatitis A virus: specific proteinase activity and RNA recognition. *J Virol.* 1997;71(3):2436–2448. doi:10.1128/jvi.71.3.2436-2448.1997
32. Mosimann SC, Cherney MM, Sia S, Plotch S, James MN. Refined X-ray crystallographic structure of the poliovirus 3C gene product. *J Mol Biol.* 1997;273(5):1032–1047. doi:10.1006/jmbi.1997.1306
33. Yang H, Yang M, Ding Y, et al. The crystal structures of severe acute respiratory syndrome virus main protease and its complex with an inhibitor. *Proc Natl Acad Sci USA.* 2003;100(23):13190–13195. doi:10.1073/pnas.1835675100

34. Chen CC, Yu X, Kuo CJ, et al. Overview of antiviral drug candidates targeting coronaviral 3C-like main proteases. *FEBS J.* 2021;288(17):5089–5121. doi:10.1111/febs.15696
35. Xiong M, Su H, Zhao W, Xie H, Shao Q, Xu Y. What coronavirus 3C-like protease tells us: from structure, substrate selectivity, to inhibitor design. *Med Res Rev.* 2021;41(4):1965–1998. doi:10.1002/med.21783
36. Cheng SC, Chang GG, Chou CY. Mutation of Glu-166 blocks the substrate-induced dimerization of SARS coronavirus main protease. *Biophys J.* 2010;98(7):1327–1336. doi:10.1016/j.bpj.2009.12.4272
37. Chen S, Hu T, Zhang J, et al. Mutation of Gly-11 on the dimer interface results in the complete crystallographic dimer dissociation of severe acute respiratory syndrome coronavirus 3C-like protease: crystal structure with molecular dynamics simulations. *J Biol Chem.* 2008;283(1):554–564. doi:10.1074/jbc.M705240200
38. Hu T, Zhang Y, Li L, et al. Two adjacent mutations on the dimer interface of SARS coronavirus 3C-like protease cause different conformational changes in crystal structure. *Virology.* 2009;388(2):324–334. doi:10.1016/j.virol.2009.03.034
39. Ferreira JC, Fadl S, Villanueva AJ, Rabeh WM. Catalytic Dyad residues His41 and Cys145 impact the catalytic activity and overall conformational fold of the main SARS-CoV-2 protease 3-chymotrypsin-like protease. *Front Chem.* 2021;9:692168. doi:10.3389/fchem.2021.692168
40. Kneller DW, Phillips G, Weiss KL, et al. Unusual zwitterionic catalytic site of SARS-CoV-2 main protease revealed by neutron crystallography. *J Biol Chem.* 2020;295(50):17365–17373. doi:10.1074/jbc.AC120.016154
41. Akaji K, Konno H. Design and evaluation of anti-SARS-coronavirus agents based on molecular interactions with the viral protease. *Molecules.* 2020;25(17):3920. doi:10.3390/molecules25173920
42. Zhang S, Krumberger M, Morris MA, et al. Structure-based drug design of an inhibitor of the SARS-CoV-2 (COVID-19) main protease using free software: a tutorial for students and scientists. *ChemRxiv.* 2020. doi:10.26434/chemrxiv.12791954
43. Kneller DW, Phillips G, O'Neill HM, et al. Structural plasticity of SARS-CoV-2 3CL M(pro) active site cavity revealed by room temperature X-ray crystallography. *Nat Commun.* 2020;11(1):3202. doi:10.1038/s41467-020-16954-7
44. Ramos-Guzmán CA, Ruiz-Pernía JJ, Tuñón I. Multiscale simulations of SARS-CoV-2 3CL protease inhibition with aldehyde derivatives. role of protein and inhibitor conformational changes in the reaction mechanism. *ACS Catal.* 2021;11(7):4157–4168. doi:10.1021/acscatal.0c05522
45. Al-Gharabli SI, Shah ST, Weik S, et al. An efficient method for the synthesis of peptide aldehyde libraries employed in the discovery of reversible SARS coronavirus main protease (SARS-CoV Mpro) inhibitors. *Chembiochem.* 2006;7(7):1048–1055. doi:10.1002/cbic.200500533
46. Yang S, Chen SJ, Hsu MF, et al. Synthesis, crystal structure, structure-activity relationships, and antiviral activity of a potent SARS coronavirus 3CL protease inhibitor. *J Med Chem.* 2006;49(16):4971–4980. doi:10.1021/jm0603926
47. Akaji K, Konno H, Mitsui H, et al. Structure-based design, synthesis, and evaluation of peptide-mimetic SARS 3CL protease inhibitors. *J Med Chem.* 2011;54(23):7962–7973. doi:10.1021/jm200870n
48. Zhu L, George S, Schmidt MF, Al-Gharabli SI, Rademann J, Hilgenfeld R. Peptide aldehyde inhibitors challenge the substrate specificity of the SARS-coronavirus main protease. *Antiviral Res.* 2011;92(2):204–212. doi:10.1016/j.antiviral.2011.08.001
49. Dai W, Zhang B, Jiang XM, et al. Structure-based design of antiviral drug candidates targeting the SARS-CoV-2 main protease. *Science.* 2020;368(6497):1331–1335. doi:10.1126/science.abb4489
50. Shie JJ, Fang JM, Kuo TH, et al. Inhibition of the severe acute respiratory syndrome 3CL protease by peptidomimetic alpha, beta-unsaturated esters. *Bioorg Med Chem.* 2005;13(17):5240–5252. doi:10.1016/j.bmc.2005.05.065
51. Zhang L, Lin D, Kusov Y, et al. Î±-ketoamides as broad-spectrum inhibitors of coronavirus and enterovirus replication: structure-based design, synthesis, and activity assessment. *J Med Chem.* 2020;63(9):4562–4578. doi:10.1021/acs.jmedchem.9b01828
52. Yang H, Xie W, Xue X, et al. Design of wide-spectrum inhibitors targeting coronavirus main proteases. *PLoS Biol.* 2005;3(10):e324. doi:10.1371/journal.pbio.0030324
53. Jin Z, Du X, Xu Y, et al. Structure of M(pro) from SARS-CoV-2 and discovery of its inhibitors. *Nature.* 2020;582(7811):289–293. doi:10.1038/s41586-020-2223-y
54. Kumar Y, Singh H, Patel CN. In silico prediction of potential inhibitors for the main protease of SARS-CoV-2 using molecular docking and dynamics simulation based drug-repurposing. *J Infect Public Health.* 2020;13(9):1210–1223. doi:10.1016/j.jiph.2020.06.016
55. Mondal D, Warshel A. Exploring the mechanism of covalent inhibition: simulating the binding free energy of Î±-ketoamide inhibitors of the main protease of SARS-CoV-2. *Biochemistry.* 2020;59(48):4601–4608. doi:10.1021/acs.biochem.0c00782
56. Zhang L, Lin D, Sun X, et al. Crystal structure of SARS-CoV-2 main protease provides a basis for design of improved Î±-ketoamide inhibitors. *Science.* 2020;368(6489):409–412. doi:10.1126/science.abb3405
57. Baig MH, Sharma T, Ahmad I, Abohashrh M, Alam MM, Dong JJ. Is PF-00835231 a Pan-SARS-CoV-2 mpro inhibitor? A comparative study. *Molecules.* 2021;26(6):1678. doi:10.3390/molecules26061678
58. de Vries M, Mohamed AS, Prescott RA, et al. A comparative analysis of SARS-CoV-2 antivirals in human airway models characterizes 3CL(pro) inhibitor PF-00835231 as a potential new treatment for COVID-19. *bioRxiv.* 2021. doi:10.1128/JVI.01819-20
59. Hoffman RL, Kania RS, Brothers MA, et al. Discovery of ketone-based covalent inhibitors of coronavirus 3CL proteases for the potential therapeutic treatment of COVID-19. *J Med Chem.* 2020;63(21):12725–12747. doi:10.1021/acs.jmedchem.0c01063
60. Fu L, Ye F, Feng Y, et al. Both Boceprevir and GC376 efficaciously inhibit SARS-CoV-2 by targeting its main protease. *Nat Commun.* 2020;11(1):4417. doi:10.1038/s41467-020-18233-x
61. Zhao Y, Fang C, Zhang Q, et al. Crystal structure of SARS-CoV-2 main protease in complex with protease inhibitor PF-07321332. *Protein Cell.* 2021;1–5. doi:10.1007/s13238-021-00883-2
62. de Vries M, Mohamed AS, Prescott RA, et al. A comparative analysis of SARS-CoV-2 antivirals characterizes 3CL(pro) inhibitor PF-00835231 as a potential new treatment for COVID-19. *J Virol.* 2021;95(10). doi:10.1128/JVI.01819-20
63. Magro G. COVID-19: review on latest available drugs and therapies against SARS-CoV-2. Coagulation and inflammation cross-talking. *Virus Res.* 2020;286:198070. doi:10.1016/j.virusres.2020.198070
64. Trujillo-Mayol I, Guerra-Valle M, Casas-Forero N, et al. Western dietary pattern antioxidant intakes and oxidative stress: importance during the SARS-CoV-2/COVID-19 pandemic. *Adv Nutr.* 2021;12(3):670–681. doi:10.1093/advances/nmaa171
65. Bermanno G, Méplan C, Mercer DK, Hesketh JE. Selenium and viral infection: are there lessons for COVID-19? *Br J Nutr.* 2021;125(6):618–627. doi:10.1017/S0007114520003128

66. Moghaddam A, Heller RA, Sun Q, et al. Selenium deficiency is associated with mortality risk from COVID-19. *Nutrients*. 2020;12(7):2098. doi:10.3390/nu12072098
67. Chang TC, Huang ML, Hsu WL, Hwang JM, Hsu LY. Synthesis and biological evaluation of ebselen and its acyclic derivatives. *Chem Pharm Bull (Tokyo)*. 2003;51(12):1413–1416. doi:10.1248/cpb.51.1413
68. Cembrzyńska-Nowak M, Szklarz E, Ingłot AD. Modulation of cytokine production by a selenoorganic compound (AE-22) in hyperreactive or hyporeactive bronchoalveolar leukocytes of asthmatics or lung cancer patients. *J Interferon Cytokine Res*. 1997;17(10):609–617. doi:10.1089/jir.1997.17.609
69. Haddad El B, McCluskie K, Birrell MA, et al. Differential effects of ebselen on neutrophil recruitment, chemokine, and inflammatory mediator expression in a rat model of lipopolysaccharide-induced pulmonary inflammation. *J Immunol*. 2002;169(2):974–982. doi:10.4049/jimmunol.169.2.974
70. Qiao Z, Wei N, Jin L, et al. The Mpro structure-based modifications of ebselen derivatives for improved antiviral activity against SARS-CoV-2 virus. *Bioorg Chem*. 2021;117:105455. doi:10.1016/j.bioorg.2021.105455
71. Batool F, Mughal EU, Zia K, et al. Synthetic flavonoids as potential antiviral agents against SARS-CoV-2 main protease. *J Biomol Struct Dyn*. 2020;1–12. doi:10.1080/07391102.2020.1850359
72. Jo S, Kim S, Kim DY, Kim MS, Shin DH. Flavonoids with inhibitory activity against SARS-CoV-2 3CLpro. *J Enzyme Inhib Med Chem*. 2020;35(1):1539–1544. doi:10.1080/14756366.2020.1801672
73. Abian O, Ortega-Alarcon D, Jimenez-Alesanco A, et al. Structural stability of SARS-CoV-2 3CLpro and identification of quercetin as an inhibitor by experimental screening. *Int J Biol Macromol*. 2020;164:1693–1703. doi:10.1016/j.ijbiomac.2020.07.235
74. Zhu Y, Xie DY. Docking characterization and in vitro inhibitory activity of flavan-3-ols and dimeric proanthocyanidins against the main protease activity of SARS-Cov-2. *Front Plant Sci*. 2020;11:601316. doi:10.3389/fpls.2020.601316
75. Xiao T, Cui M, Zheng C, et al. Myricetin inhibits SARS-CoV-2 viral replication by targeting M(pro) and ameliorates pulmonary inflammation. *Front Pharmacol*. 2021;12:669642. doi:10.3389/fphar.2021.669642
76. Xiao T, Wei Y, Cui M, et al. Effect of dihydromyricetin on SARS-CoV-2 viral replication and pulmonary inflammation and fibrosis. *Phytomedicine*. 2021;91:153704. doi:10.1016/j.phymed.2021.153704
77. Chiou WC, Lu HF, Hsu NY, et al. Ugonin J acts as a SARS-CoV-2 3C-like protease inhibitor and exhibits anti-inflammatory properties. *Front Pharmacol*. 2021;12:720018. doi:10.3389/fphar.2021.720018
78. Uras IS, Ebada SS, Korinek M, et al. Anti-inflammatory, antiallergic, and COVID-19 main protease (M(pro)) inhibitory activities of butenolides from a marine-derived fungus *Aspergillus terreus*. *Molecules*. 2021;26(11):3354. doi:10.3390/molecules26113354
79. Shi TH, Huang YL, Chen CC, et al. Andrographolide and its fluorescent derivative inhibit the main proteases of 2019-nCoV and SARS-CoV through covalent linkage. *Biochem Biophys Res Commun*. 2020;533(3):467–473. doi:10.1016/j.bbrc.2020.08.086
80. Choudhary OP, Dhawan M. Omicron variant (B.1.1.529) of SARS-CoV-2: threat assessment and plan of action-correspondence. *Int J Surg*. 2021;97:106187. doi:10.1016/j.ijssu.2021.106187
81. Mannar D, Saville JW, Zhu X, et al. SARS-CoV-2 Omicron variant: antibody evasion and cryo-EM structure of spike protein-ACE2 complex. *Science*. 2022;375(6582):760–764. doi:10.1126/science.abn7760
82. Ullrich S, Ekanayake KB, Otting G, Nitsche C. Main protease mutants of SARS-CoV-2 variants remain susceptible to nirmatrelvir. *Bioorg Med Chem Lett*. 2022;62:128629. doi:10.1016/j.bmcl.2022.128629
83. Zhang L, Li Q, Liang Z, et al. The significant immune escape of pseudotyped SARS-CoV-2 variant omicron. *Emerg Microbes Infect*. 2021;11:1–11.
84. Chen P, Nirula A, Heller B, et al. SARS-CoV-2 neutralizing antibody LY-CoV555 in outpatients with Covid-19. *N Engl J Med*. 2021;384(3):229–237. doi:10.1056/NEJMoa2029849
85. Corti D, Purcell LA, Snell G, Tackling VD. COVID-19 with neutralizing monoclonal antibodies. *Cell*. 2021;184(12):3086–3108. doi:10.1016/j.cell.2021.05.005
86. Tuccori M, Ferraro S, Convertino I, et al. Anti-SARS-CoV-2 neutralizing monoclonal antibodies: clinical pipeline. *mAbs*. 2020;12(1):1854149. doi:10.1080/19420862.2020.1854149
87. Seeliger D, de Groot BL. Ligand docking and binding site analysis with PyMOL and Autodock/Vina. *J Comput Aided Mol Des*. 2010;24(5):417–422. doi:10.1007/s10822-010-9352-6

Drug Design, Development and Therapy

Dovepress

Publish your work in this journal

Drug Design, Development and Therapy is an international, peer-reviewed open-access journal that spans the spectrum of drug design and development through to clinical applications. Clinical outcomes, patient safety, and programs for the development and effective, safe, and sustained use of medicines are a feature of the journal, which has also been accepted for indexing on PubMed Central. The manuscript management system is completely online and includes a very quick and fair peer-review system, which is all easy to use. Visit <http://www.dovepress.com/testimonials.php> to read real quotes from published authors.

Submit your manuscript here: <https://www.dovepress.com/drug-design-development-and-therapy-journal>